Pulse-propagation-induced higher orders of diffraction in transient four-wave mixing with semiconductors

B. Lummer, J.-M. Wagner, R. Heitz, A. Hoffmann, and I. Broser

Institut für Festkörperphysik, Technische Universität Berlin, Hardenbergstraße 36, 10623 Berlin, Germany

R. Zimmermann

Max-Planck-Gesellschaft, Arbeitsgruppe ''Halbleitertheorie'' an der Humboldt-Universität zu Berlin,

Hausvogteiplatz 5-7, 10117 Berlin, Germany

Higher orders of diffraction observed in a transient four-wave mixing experiment with acceptor-bound exciton complexes in CdS are analyzed in terms of pulse propagation. The description is based on a mean-field correction to the driving electric field in the optical Bloch equations, which are shown to generally lack higher-order diffraction for two-pulse self-diffraction. A propagation-induced sequence of stimulated echoes diffracted at the population grating dominates at least the second order of diffraction. [S0163-1829(96)07147-0]

I. INTRODUCTION

Transient four-wave mixing (TFWM) has been proven to be a powerful tool for the investigation of the coherent dynamics of excitations in semiconductors.[1] In the self-diffraction geometry of TFWM (Fig. 1), the nonlinear polarization generated by the two incident pulses ($\mathbf{k}_1$ and $\mathbf{k}_2$) of equal frequency separated by a delay τ gives rise to diffracted light with wave vector $\mathbf{k}_2 + n(\mathbf{k}_2 - \mathbf{k}_1)$. Higher orders of diffraction, denoted by wave vectors with $n > 1$, occur for a variety of reasons. Multiwave mixing and consecutive lower-order processes (known as cascading processes[2]) have been demonstrated in gaseous[3,4] and condensed matter systems[5,6] under cw excitation. Nonsinusoidal gratings generated by diffusion[7] or by saturation[8] as well as the coherent exciton-exciton interaction[9] have been cited to explain higher-order diffracted signals observed in TFWM. The simultaneous action of these processes often makes the evaluation of experimental results ambiguous.

The analysis of TFWM results is based on the optical[10] (OBE) or (in case of a semiconductor) the semiconductor[11] (SBE) Bloch equations, describing a system of noninteracting and Coulomb-correlated two-level absorbers, respectively. In transient FWM, the OBE give rise to signal exclusively in the first order of diffraction,[12] whereas many-body interactions (SBE) result in higher-order diffracted signals.[13] Pulse propagation through the sample is neglected within these approaches, but can be taken into account by coupling Maxwell's equation with the OBE or the SBE describing the specific microscopic system.

Pulse propagation can have several consequences for TFWM experiments, e.g., a strong influence of the absorption strength on the coherent decay,[14] multiple photon echoes,[8,15] signals for negative delay times,[16] or interference effects for strongly dispersive excitonic polaritons in semiconductors.[17,18] However, the significance of pulse propagation for TFWM has not been universally appreciated but warrants further investigation since it provides an inevi-

table coupling mechanism between the absorbing centers. Especially, the substantial effect of pulse propagation becomes most obvious from the occurrence of higher-order diffracted signals (or equivalently multiple photon echoes[8,15]) even at low and moderate optical densities.

In the present paper, higher orders of diffraction observed in TFWM experiments with the neutral-acceptor-bound exciton (A^0, X) in CdS are analyzed. By comparison of the experimental data to a simplified model for pulse propagation it is shown that these higher-order signals result from a propagation-induced sequence of stimulated echoes. Thereby, our experiment renders the possibility to study exclusively the effects of pulse propagation on the TFWM process in a semiconductor.

II. EXPERIMENTAL RESULTS

Recently, we have published TFWM results at the (A^0, X) complex in CdS in which the first-order diffracted signal[19] was considered. Here, the investigation is extended to the second order. At 1.8 K a 15-μm-thick CdS sample has been excited with narrow-bandwidth 2-ps pulses exciting resonantly the neutral-acceptor-bound exciton complexes at 2.5356 eV. Figure 2 shows the time-integrated (TI) and time-resolved (TR) FWM signals, illustrating the basic properties of the first- and second-order diffracted signal. The TI second-order signal [$n = 2$ in Fig. 2(a)] reveals a correlation
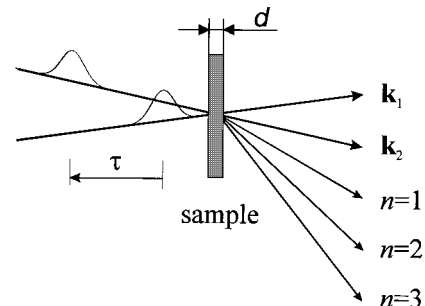

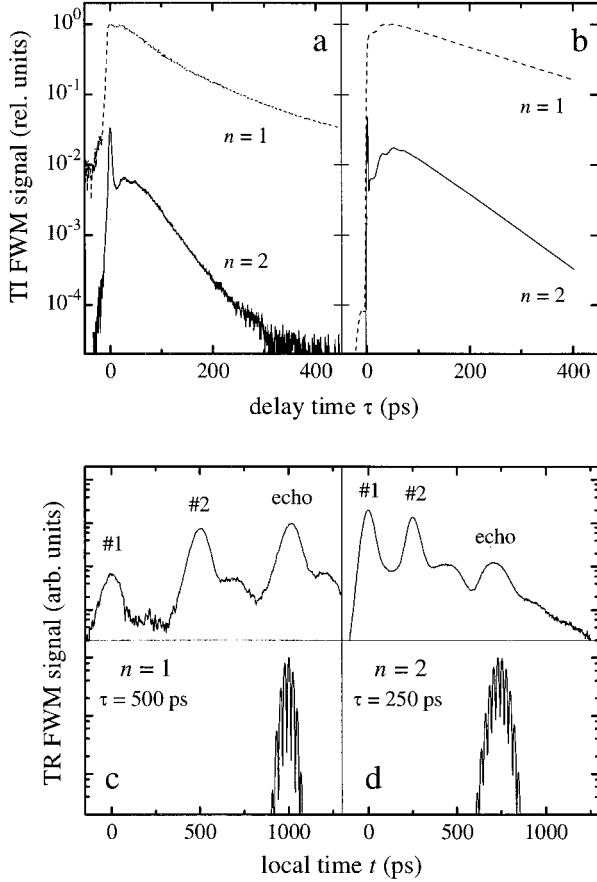FIG. 1. Scheme of the self-diffraction geometry.

FIG. 2. Experimental TI and TR FWM signals [(a) and upper parts of (c) and (d)] for the (A^0,X) complex in CdS at $T=1.8$ K in comparison to TFWM signals calculated from MFA. #1 and #2 refer to contributions from the incident Rayleigh-scattered pulses at $t=0$ and $t=\tau$. The curves in (a) and (b) are normalized to the maximum value of the curve for $n=1$.

peak at $\tau=0$ and shows a slight rise for small delay times. It decays by a factor of 2.5 faster than the first-order one ($n=1$). The nonexponential decay of the experimental signal can be explained by residual free exciton scattering.[19,20] The photon echo in second order occurs at approximately 3τ instead of 2τ in first order [Figs. 2(c) and 2(d) upper parts, respectively]. A temporal width of 80 ps for the $n=2$ echo is estimated whereas for $n=1$ it is limited by the experimental time resolution of 60 ps.

In the following, we are interested in a comparison of the first- and second-order diffracted signals rather than to consider the peculiarities of bound excitons. This has been done in Refs. 19 and 20.

III. MODEL

Due to many-body interactions, most semiconductor systems studied in FWM experiments are quite complex to describe. In contrast, bound excitons as localized excitations in a semiconductor can be expected to behave like independent two-level absorbers at sufficiently low defect concentrations. Interactions with free excitons and phonons become important only at high excitation densities or elevated sample temperatures.[19,20] Thus, the bound excitons are adequately

described by the OBE with inhomogeneously distributed eigenfrequencies. However, the OBE alone do explain the first order of diffraction only but do not give rise to signals in higher orders of diffraction. To understand this, consider the OBE for a two-level system driven by the optical field $F(t)=\mu E(\mathbf{r},t)/\hbar$ (μ is the dipole moment). They determine the temporal evolution of the upper level occupation ($\mathcal{N}$) and the complex polarization (Ψ):

$$\left[\partial_t+\frac{1}{T_1}\right]\mathcal{N}=-i(\Psi F^*-\Psi^* F), \qquad (1a)$$

$$\left[\partial_t+\frac{1}{T_2}+i(\Omega-\omega)\right]\Psi=i(1-2\mathcal{N})F, \qquad (1b)$$

where ω is the center frequency of the exciting light pulse, $\hbar\Omega$ is the energy separation of the two levels, T_1 is the lifetime, T_2 the dephasing time, and the rotating-wave approximation has been used.

For the typical TFWM experiment, the excitation consists of two pulses propagating in different directions,

$$F(t)=F_1(t)\exp(i\mathbf{k}_1\cdot\mathbf{r})+F_2(t)\exp(i\mathbf{k}_2\cdot\mathbf{r}), \qquad (2)$$

with real envelopes $F_j(t)$. Thus, a Fourier expansion with respect to the momentum difference (grating vector) $\mathbf{k}_g=\mathbf{k}_2-\mathbf{k}_1$ is useful,

$$\mathcal{N}=\sum_{m=-\infty}^{\infty}\mathcal{N}_m\exp(im\mathbf{k}_g\cdot\mathbf{r}), \qquad (3a)$$

$$\Psi=i\exp(i\mathbf{k}_2\cdot\mathbf{r})\sum_{m=-\infty}^{\infty}\Psi_m\exp(im\mathbf{k}_g\cdot\mathbf{r}). \qquad (3b)$$

Equating coefficients gives

$$\left[\partial_t+\frac{1}{T_1}\right]\mathcal{N}_m=(\Psi_{m-1}+\Psi_{-m-1}^*)F_1+(\Psi_m+\Psi_{-m}^*)F_2, \qquad (4a)$$

$$\left[\partial_t+\frac{1}{T_2}+i(\Omega-\omega)\right]\Psi_m=(\delta_{m,-1}-2\mathcal{N}_{m+1})F_1$$
$$+(\delta_{m,0}-2\mathcal{N}_m)F_2. \qquad (4b)$$

Obviously, $\mathcal{N}_m^*=\mathcal{N}_{-m}$ holds, which proves the real value of the density $\mathcal{N}$. We assume that pulse F_1 comes first, with no temporal overlap with F_2. Before arrival of the second pulse, only the coefficients Ψ_{-1} and $\mathcal{N}_0$ are excited. During and after the second pulse we have $F_1=0$, and the coefficients obey

$$\left[\partial_t+\frac{1}{T_1}\right]\mathcal{N}_m=(\Psi_m+\Psi_{-m}^*)F_2, \qquad (5a)$$

$$\left[\partial_t+\frac{1}{T_2}+i(\Omega-\omega)\right]\Psi_m=(\delta_{m,0}-2\mathcal{N}_m)F_2. \qquad (5b)$$

Additionally to the field F_2, the quantities Ψ_{-1} and $\mathcal{N}_0$ as generated by the first pulse act as source terms. By an iterative argument it can be seen that only the subset

$$\Psi_{-1}, \quad \Psi_0, \quad \Psi_{+1}, \quad \mathcal{N}_{-1}, \quad \mathcal{N}_0, \quad \mathcal{N}_{+1} \qquad (6)$$

has nonzero values. Going back to the original definition we realize that polarizations are generated only in the directions $\mathbf{k}_1$, $\mathbf{k}_2$ (input) and $2\mathbf{k}_2 - \mathbf{k}_1$ (first order of diffraction). The argument given above did not use an expansion in the field strengths (χ_3), thus extending earlier proofs of the absence of higher-order diffraction within the OBE.[12] If both pulses overlap, however, additional source terms driven by F_1 are present, and higher orders can be excited.

This shows that in the transient case only four-wave mixing is possible in the OBE, and that higher-order wave mixing processes occur only for coinciding pulses. We wish to emphasize that this result is obtained for the case of a single pair of coherent pulses. In the work of Silberberg *et al.*[8] higher-order wave mixing occurs due to saturation obtained in an accumulated experiment (with about 10^6 pulse pairs during T_1), where a stationary state can be assumed.

In view of the transient behavior of the OBE our experimental results are somewhat surprising. To explain the second order of diffraction there has to be a phase-preserving interaction among the bound excitons. While for strongly localized bound excitons a coherent interaction such as the many-particle Coulomb interaction between free excitons[11] is not expected, the most natural effect to consider is pulse propagation in the sample. The (classical) electric field propagates along the z axis and is taken to be linearly polarized in the x direction. Within the rotating-wave and the slowly varying envelope approximation, the wave equation for the electric field E driven by the polarization P reads in the coordinates[21] $t' = t - z/c$ (local time) and $z' = z$

$$\partial_{z'}E = \frac{i}{2}\frac{k}{\epsilon_0 \epsilon_b}P, \tag{7}$$

with c the speed of light and k the wave number in the medium. The background susceptibility ϵ_b is assumed to be nondispersive. For convenience, we will drop the prime henceforth.

The macroscopic polarization P is given by

$$P = N\mu^*\langle\Psi\rangle, \tag{8}$$

with N the density of absorbing centers. The polarization Ψ is taken from the OBE and the brackets denote the average over the (normalized) inhomogeneous distribution g, which is assumed to be without any correlation among the different eigenfrequencies.

A numerical solution of the Maxwell optical Bloch equations (MOB) requires extensive computing time. However, attractive predictions can be obtained by an approximate treatment of Eq. (7) as done in a similar way in Ref. 16. For moderate absorption, the weak spatial dependence allows one to treat E and P as linear functions of z around the sample center. Thus, the spatial dependence is removed entirely, and the average field $F = \mu E/\hbar$ within the sample of thickness d is related to the input and output fields by

$$F = F_{\text{in}} + iL\langle\Psi\rangle, \quad F_{\text{out}} = F + iL\langle\Psi\rangle, \tag{9}$$

with the imaginary coupling coefficient

$$iL = \frac{ikdN|\mu|^2}{4\epsilon_0\epsilon_b\hbar}. \tag{10}$$

Equation (9) shows that, as a result of propagation, the driving field F in the optical Bloch equations is the incoming electric field F_{in} corrected by an effective mean field arising from the sample polarization. This accounts for the contribution of the reradiated fields to the excitation within the sample.

The linear absorption of an inhomogeneously broadened two-level medium is given by $\alpha(\omega) = \int\alpha_\Omega(\omega)d\Omega$, and with

$$\int \alpha_\Omega(\omega) \, d\omega = \frac{N_\Omega|\mu|^2\Omega}{\epsilon_0\epsilon_b\hbar c}\pi \tag{11}$$

[where $N_\Omega = Ng(\Omega)$], L is related to the integrated linear absorption by

$$L = \frac{d}{4\pi}\int \alpha(\omega) \, d\omega, \tag{12}$$

if the width of the spectral line is assumed to be small compared to that of the exciting light pulse. Within the mean-field approximation (MFA) described above, Eqs. (1) read

$$\left[\partial_t + \frac{1}{T_1}\right]\mathcal{N} = 2\text{Im}(\Psi F_{\text{in}}^*) - 2L\text{Re}(\Psi\langle\Psi\rangle^*), \tag{13a}$$

$$\left[\partial_t + \frac{1}{T_2} + i(\Omega - \omega)\right]\Psi = (1 - 2\mathcal{N})(iF_{\text{in}} - L\langle\Psi\rangle). \tag{13b}$$

The additional L-dependent terms stem from the propagation and describe the reabsorption of the fields emitted by the sample polarization. They act as a feedback mechanism in the OBE, giving the possibility to diffract not only the input pulses but also the reradiated fields. Equations (13) therefore describe an ensemble of self-interacting two-level systems.

To calculate the TFWM signal Eqs. (13) are solved numerically for a pair of Gaussian input pulses separated by a delay τ. The number of oscillators representing the Gaussian inhomogeneous distribution (full width at half maximum $\hbar\Delta\Omega$) is chosen sufficiently large so as not to influence the obtained signal. Within this treatment, the *total* polarization in the sample is calculated without being restricted to weak fields as in perturbation approximation.[16] A Fourier transformation of the output [Eq. (9)] with respect to the relative phase of the incoming pulses allows a separation of the different diffraction orders. To this end, a phase factor is attached to the second pulse: $F_{\text{in}}(t) = F_1(t) + F_2(t - \tau)\exp(i\varphi)$, and Eqs. (13) are solved numerically for different phases φ.

IV. DISCUSSION

The modeling aims to explain our experimental results for acceptor-bound excitons in CdS. Thus, for the energy and phase relaxation times as well as for the inhomogeneous broadening, typical parameters of this system[19] are used throughout this paper ($T_1 = 1000$ ps, $T_2 = 800$ ps, $\hbar\Delta\Omega = 45$ μeV). Furthermore, an excitation pulsewidth of 2 ps and an $F^{\text{peak}} = 0.35$ ps^{-1} for both pulses are chosen in accordance with the experiment.

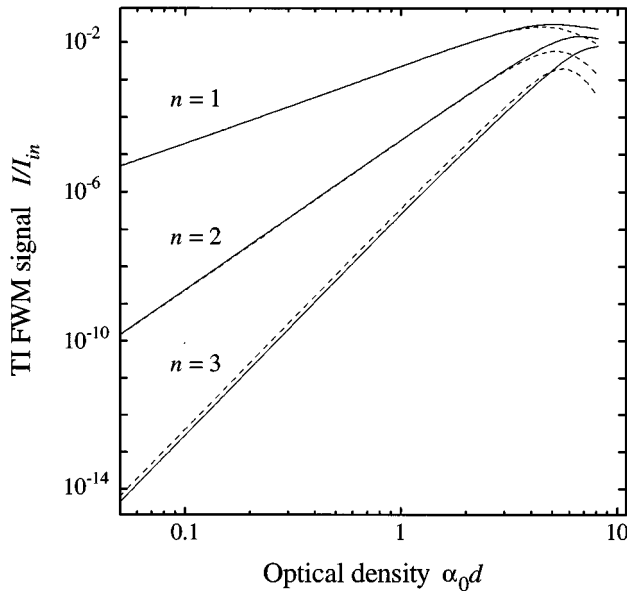Figure 3 shows the TI FWM signal for a delay time

FIG. 3. Calculated TI FWM signal at $\tau = 100$ ps as a function of the peak optical density $\alpha_0 d \propto L$ for various orders of diffraction. Solid curves: MOB, dashed curves: MFA.

$\tau = 100$ ps as a function of the peak optical density $\alpha_0 d$, for the first, second, and third order of diffraction, calculated in the MFA and, for comparison, by the complete numerical treatment of propagation (MOB). In the latter, the coupled Maxwell [Eq. (7)] and optical Bloch equations [Eqs. (1)] have been solved, keeping the full temporal and spatial dependence. As obvious from Fig. 3, an increasing $\alpha_0 d$ drastically increases the signal strength in the higher orders of diffraction. For $\alpha_0 d = 4$, the signal in the second order is only a factor of 3 smaller than in first order and should therefore be easily observed in experiment. The crucial parameter for the validity of the MFA is the peak optical density. Figure 3 shows that the MFA holds for $\alpha_0 d$ up to 3. For the chosen set of parameters, this compares to $L = 10$ μeV/$\hbar$.

Figure 4(a) shows the decay of the TI signals in the first three orders ($n = 1,2,3$) of diffraction derived from the MFA. The decay of the signal accelerates with increasing order and a correlation peak appears around zero delay. Additionally, one notes a substantial influence of T_1 on the decay in second and third order (dashed curves). Figure 4(b) shows the corresponding TR FWM signals at a fixed pulse delay of 200 ps. In each order n a photon echo is generated at times $t_n = (n+1)\tau$ with increasing width. A detailed observation renders the photon echoes to peak slightly before $(n+1)\tau$. This is due to shaping by the superimposed polarization decay.

Two basic processes arising from pulse propagation lead to higher orders of diffraction. Any pulse that travels through the sample can interact with the polarizations and population gratings present therein. The resonant interaction with a polarization leads to self-diffraction of the pulse, whereas interaction with a population grating gives rise to a stimulated echo for inhomogeneous broadening.

As the first echo pulse propagates through the sample in direction $2\mathbf{k}_2 - \mathbf{k}_1$, the interaction with the polarizations es-
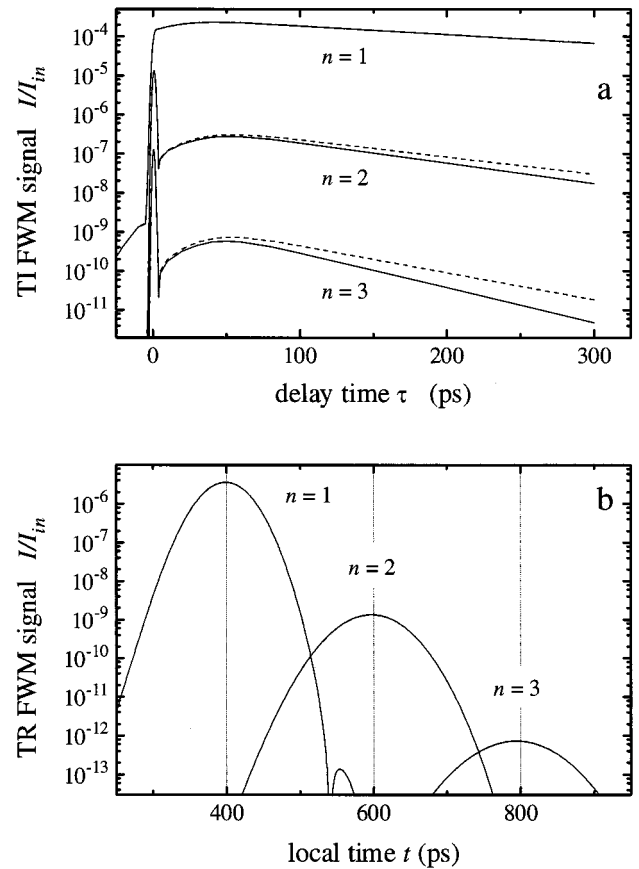

FIG. 4. TFWM signals for $\alpha_0 d = 0.3$ calculated from MFA for $T_1 = 1000$ ps (solid curves) and $T_1 = 10\,000$ ps (dashed curves). For the TR FWM signal in (b) $\tau = 200$ ps is chosen.

tablished from pulse $\mathbf{k}_2$ and $\mathbf{k}_1$ results in self-diffraction into directions $3\mathbf{k}_2 - 2\mathbf{k}_1$ and $4\mathbf{k}_2 - 3\mathbf{k}_1$, with a photon echo at $t = 3\tau$ and $t = 4\tau$, respectively. This consecutive FWM creates a higher Fourier component in the population grating at $t = 2\tau$ and is completely analogous to the formation of the first echo through the second excitation pulse. On the other hand, the interaction of the first echo pulse with the grating generated by the two incident pulses stimulates a photon echo at 3τ in the direction $3\mathbf{k}_2 - 2\mathbf{k}_1$. The repetition of this process gives rise to a sequence of stimulated echoes where each order n drives the order $n+1$. Note that this is a coherent transient version of continued diffraction as described in Ref. 22. However, no coupling into order $n-1$ occurs.

Both the consecutive FWM and the echo sequence, as well as their combinations, contribute to the nth order of diffraction for $n \geq 2$ and cannot be easily distinguished. However, there is a fundamental physical difference between these two processes: Since the sequence of stimulated echoes arises from diffraction by gratings generated earlier, the decay time of this process has to depend on T_1, whereas consecutive FWM is independent on T_1.

To discuss the second order of diffraction in more detail, one notes that here the stimulated echo is to the fifth order in the fields, and consecutive FWM represents a seventh-order process. Expanding Eqs. (13) up to the seventh order in the fields, we find the decay rate of both processes to be

$$\Gamma^{(n=2)}_{\text{stimulated}} = \frac{8}{T_2} + \frac{2}{T_1}, \quad \Gamma^{(n=2)}_{\text{cons.FWM}} = \frac{12}{T_2}, \qquad (14)$$

respectively. From a comparison with Fig. 4(a), the decay for $n=2$ is given by $\Gamma^{(n=2)}_{\text{stimulated}}$. Therefore, we conclude that the echo sequence dominates at least the second order of diffraction. This is further supported by the fact that the echo sequence leads to a $(\alpha_0 d)^{2n}$ dependence for small $\alpha_0 d$, as depicted in Fig. 3.

For the actual modeling of the TFWM signals [Figs. 2(b) and (c) and (d) lower parts], besides the above given parameters we have to take into account that the sample shows two absorption lines with energy splitting $\Delta E = 175$ μeV, corresponding to different acceptors. The absorption profile is fitted with two Gaussians ($\alpha_0 d$ of 1.18 and 0.86, full width at half maximum $\hbar \Delta \Omega = 45$ μeV) giving a total L of 7.8 μeV/$\hbar$ well within the validity of the MFA. In addition to the experimental data in Fig. 2 the result of the modeling with the MFA is depicted. All charcteristic features are well reproduced, and we find a fairly good agreement between the model and the experiment:

a. The correlation peak. It arises from the fact that at pulse overlap the second input pulse itself is instantaneously diffracted into $n=2$ from the generated higher-order grating.

b. The echo position. The echo appears at $(n+1)\tau$ in the nth order with a slight shift to smaller t caused by the shaping with the polarization decay. This shift is seen in both experimental and modeled data.

c. The accelerated decay of the TI signal in second order. Equation (14) predicts with $\Gamma^{(n=2)}_{\text{stimulated}}$ a factor of 2.4 as the ratio of the ascents between first and second order ($T_1 = 1000$ ps, $T_2 = 800$ ps, $\Gamma^{(n=1)} = 4/T_2$). This is in very good agreement to the experimental ratio of 2.5 and proves that the observed second order diffracted signal is predominantly caused by the propagation-induced sequence of stimulated echoes as described above.

d. The width of the echo. Whereas the first-order echo is driven by the short input pulse, the second-order echo is driven by the first-order one and consequently has an increased temporal width.

e. The intensity ratio between first and second order. As depicted in Fig. 3 the intensity ratio is a direct measure of the optical thickness of the sample.

f. The modulation of the signal. The simultaneous excitation of both spectral components causes a modulation of the TFWM signals due to polarization interference.[23] This modulation is apparent in both experimental and calculated TFWM signals except for the TR measurement [Figs. 2(c) and 2(d) upper parts] because of the limited time resolution.

V. CONCLUSION

In conclusion, we have demonstrated that higher orders of diffraction in a transient four-wave-mixing experiment with acceptor-bound exciton complexes in CdS are caused by pulse propagation. The echo in the second order of diffraction arises predominantly from a propagation-induced feedback: The first-order echo pulse stimulates an echo diffracted by the population grating established by the incident pulses. For not too strong absorption, propagation is adequately described by a mean-field correction to the driving electric field in the optical Bloch equations. The accelerated decay of the observed second-order signal and the relative strength between first and second order as well as the photon echo appearing at 3τ and its increased temporal width are well explained by the mean-field concept.

The described properties of the higher-order signals have been deduced from a mean-field correction for the electric field, leading to equations with a local-field-like structure. Thus, any interaction that can be described within a local-field formalism (e.g., Coulomb interaction among excitons[11]) should result in higher-order signals with similar properties. Corresponding studies are currently under way.

[1] E. O. Göbel, in *Festkörperprobleme/Advances in Solid State Physics*, Vol. 30, edited by U. Rössler (Vieweg, Braunschweig, 1990), p. 269; J. M. Hvam, in *Nonlinear Spectroscopy of Solids*, Vol. 339 of *NATO Advanced Studies Institute Series B: Physics*, edited by B. Di Bartolo (Plenum Press, New York, 1994).

[2] C. Flytzanis, in *Quantum Electronics*, edited by H. Rabin and C. L. Tang (Academic, New York, 1975), Vol. I, Pt. A.

[3] R. Trebino and L. A. Rahn, Opt. Lett. **12**, 912 (1987).

[4] N. Tan-no, K. Ohkawara, and H. Inaba, Phys. Rev. Lett. **46**, 1282 (1981).

[5] H. J. Eichler, P. Günter, and D. W. Pohl, *Laser Induced Dynamic Gratings*, Springer Series in Optical Sciences Vol. 50 (Springer, Berlin, 1986).

[6] A. Maruani, J. L. Oudar, E. Batifol, and D. S. Chemla, Phys. Rev. Lett. **41**, 1372 (1978); D. S. Chemla, A. Maruani, and F. Bonnouvrier, Phys. Rev. A **26**, 3026 (1982).

[7] H. Saito and A. Watanabe, Phys. Rev. B **37**, 10 236 (1988); B. P. McGinnis, E. M. Wright, S. W. Koch, and N. Peyghambarian, Phys. Rev. A **41**, 523 (1990).

[8] Y. Silberberg, V. L. da Silva, J. P. Heritage, E. W. Chase, and M. J. Andrejco, IEEE J. Quantum Electron. **28**, 2369 (1992).

[9] A. J. Fischer, D. S. Kim, J. Hays, W. Shan, J. J. Song, D. B. Eason, J. Ren, J. F. Schetzina, H. Luo, J. K. Furdyna, Z. Q. Zhu, T. Yao, J. F. Klem, and W. Schäfer, Phys. Rev. Lett. **73**, 2368 (1994).

[10] L. Allen and J. H. Eberly, *Optical Resonance and Two-Level Atoms* (Wiley, New York, 1975); T. Yajima and Y. Taira, J. Phys. Soc. Jpn. **47**, 1620 (1979).

[11] M. Lindberg and S. W. Koch, Phys. Rev. B **38**, 3342 (1988); M. Wegener, D. S. Chemla, S. Schmitt-Rink, and W. Schäfer, Phys. Rev. A **42**, 5675 (1990).

[12] S. Wu, X.-C. Zhang, and R. L. Fork, Appl. Phys. Lett. **61**, 919 (1992).

[13] A. Schulze, A. Knorr, P. Thomas, and S. W. Koch, Solid State Commun. **94**, 911 (1995).

[14] R. W. Olson, H. W. H. Lee, F. G. Patterson, and M. D. Fayer, J. Chem. Phys. **76**, 31 (1982); O. Kinrot and Y. Prior, Phys. Rev. A **50**, 1999 (1994).

[15] I. D. Abella, N. A. Kurnit, and S. R. Hartmann, Phys. Rev. **141**,

391 (1966); B. Gross and J. T. Manassah, Laser Physics **3**, 612 (1993).

[16] M. N. Belov, E. A. Manykin, and M. A. Selifanov, Opt. Commun. **99**, 101 (1993).

[17] P. Schillak and I. Balslev, Phys. Rev. B **48**, 9426 (1993).

[18] A. Schulze, A. Knorr, and S. W. Koch, Phys. Rev. B **51**, 10 601 (1995).

[19] R. Heitz, B. Lummer, A. Hoffmann, and I. Broser, J. Lumin. **58**, 237 (1994).

[20] H. Schwab, V. G. Lyssenko, and J. M. Hvam, Phys. Rev. B **44**, 3999 (1991).

[21] A. Icsevgi and W. E. Lamb, Jr., Phys. Rev. **185**, 517 (1969).

[22] H. L. Fragnito, S.F. Pereira, and A. Kiel, J. Opt. Soc. Am. B **4**, 1309 (1987).

[23] K.-H. Pantke and J. M. Hvam, Int. J. Mod. Phys. B **8**, 73 (1994).